10 Neutrino Oscillations

10.1 Neutrino mixing

Particles are produced in interactions. The interaction process defines the properties of the emitted particle, for example it is a photon or an axion.

Depending on the medium in which these particles propagate, these interaction eigenstates may not coincide with the propagation eigenstates—the effective mass basis may be different from the interaction basis.

This situation arises for all fermions (quarks and neutrinos). They are fundamentally massless and they are usually produced in interactions involving gauge interactions. On the other hand, they acquire a mass ultimately through their interaction with a Higgs field: Need not be diagonal in the same basis.

For the charged leptons we define the electron to be the charged lepton with the smallest mass, the muon the next one, and the τ lepton the heaviest one.

Neutrinos are typically produced in charged-current reactions, schematically of the form

$$\begin{aligned} &e^- + p \to n + \nu_e \\ &\mu^- + p \to n + \nu_\mu \\ &\tau^- + p \to n + \nu_\tau \end{aligned}$$

By definition we call a ν_e the particle that arises in combination with the disappearance of an electron (or the production of a positron). These are the interaction eigenstates—they are defined by the interaction (or process) by which they are produced.

More fundamentally, the interaction eigenstates are defined by the interaction vertex with the W boson that mediates charged current interactions:

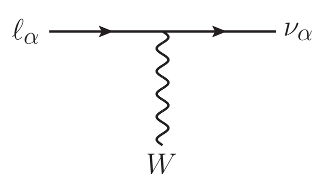

If neutrinos have non-vanishing masses, one does not know a priori if in vacuum ν_e propagates with a given mass or if it is a superposition of all three mass eigenstates: The "polarization" in flavor space defined by the interaction with charged leptons need not coincide with the propagation eigenstates.

The electron neutrino state, for example, in general is a superposition of the mass eigenstates with masses m_1, m_2 and m_3 of the form

$$|\nu_e\rangle = \mathsf{U}^*_{e1}|\nu_1\rangle + \mathsf{U}^*_{e2}|\nu_2\rangle + \mathsf{U}^*_{e3}|\nu_3\rangle$$

Or conversely for any mass eigenstate

$$|\nu_i\rangle = \sum_{\alpha=e,\mu,\tau} \mathsf{U}_{i\alpha}|\nu_\alpha\rangle \qquad \text{for} \qquad i=1,2,3$$

The 3×3 matrix U describes neutrino flavor mixing. It is sometimes called the leptonic mixing matrix or the PMNS matrix after Pontecorvo, Maki, Nakagawa, and Sakata.

Completely analogous reasoning applies to the quarks where the mixing matrix is known as the Cabbibo-Kobayashi-Maskawa matrix. Flavor mixing among quarks has been known for a long time. However, for neutrinos the mixing angles are much larger, the mass differences much smaller. For neutrinos the oscillation effects are of macroscopic and even astronomical interest.

As already discussed for axion-photon mixing, for a two-flavor system the mixing matrix is a simple rotation in flavor space

$$\mathsf{U} = \begin{pmatrix} \cos\theta & \sin\theta \\ -\sin\theta & \cos\theta \end{pmatrix}$$

determined by the mixing angle θ.

However, reality is more complicated because we have three flavors and therefore U is a 3×3 matrix. Many representations are possible. Commonly built up from three Euler rotations and three complex phases in the form

$$\mathsf{U} = \begin{pmatrix} c_{12} & s_{12} & 0 \\ -s_{12} & c_{12} & 0 \\ 0 & 0 & 1 \end{pmatrix} \begin{pmatrix} c_{13} & 0 & s_{13}\mathrm{e}^{-\mathrm{i}\delta} \\ 0 & 1 & 0 \\ -s_{13}\mathrm{e}^{\mathrm{i}\delta} & 0 & c_{13} \end{pmatrix} \begin{pmatrix} 1 & 0 & 0 \\ 0 & c_{23} & s_{23} \\ 0 & -s_{23} & c_{23} \end{pmatrix} \begin{pmatrix} \mathrm{e}^{\mathrm{i}\alpha_1} & 0 & 0 \\ 0 & \mathrm{e}^{\mathrm{i}\alpha_2} & 0 \\ 0 & 0 & 1 \end{pmatrix}$$

where $s_{12} = \sin(\theta_{12})$, $c_{12} = \cos(\theta_{12})$ and so forth. The mixing angles take values in the range $0 \le \theta_{ab} \le \pi/2$ whereas the "Dirac phase" varies in the range $0 \le \delta \le 2\pi$.

The "Majorana phases" α_1 and α_2 can be removed in the Dirac case by a re-definition of the fields, whereas in the Majorana case they are relevant for neutrinoless double-beta decay. For oscillations they never play a role and we will drop them henceforth.

10.2 Main facts about neutrino mass and mixing parameters

Neutrino oscillations have been observed in many systems and many channels (to be discussed in more detail below). They reveal the following facts about neutrino masses and mixing parameters.

10.2.1 Mixing angles

The mixing angle θ_{12} has been measured in the oscillations of solar and reactor neutrinos (in degrees), see http://arxiv.org/abs/1001.4524

$$\theta_{12} = 34.4 \pm 1.0 \ \left({}^{+3.2}_{-2.9}\right) \qquad \text{at } 1\,\sigma\text{, in brackets } 3\,\sigma$$

This is compatible with 35.26°, i.e. with the simple values

$$\tan^2\theta_{12} = \frac{1}{2} \qquad \text{or} \qquad s_{12} = \frac{1}{\sqrt{3}}$$

This mixing angle is not small. It is often called the "solar mixing angle" $\theta_\odot$ because it dominates solar neutrino oscillations.

The mixing angle θ_{23} first showed up in atmospheric neutrino oscillations and thus is often called the "atmospheric mixing angle" $\theta_{\rm atm}$

$$\theta_{23} = 42.3^{+5.3}_{-2.8} \ \left({}^{+11.4}_{-7.1}\right)$$

This is compatible with 45°, i.e. with the simple value

$$s_{23} = \frac{1}{\sqrt{2}}$$

This represents maximal mixing.

The mixing angle θ_{13} is constrained mainly by reactor neutrino experiments, notably the CHOOZ experiment and is therefore sometimes called the CHOOZ angle

$$\theta_{13} = 6.8^{+2.6}_{-3.6} \ (< 13.2) \qquad \text{or} \qquad s_{13}^2 = 0.014^{+0.013}_{-0.011} \ (< 0.052)$$

In other words, at reasonable significance there is only an upper limit and this angle could still vanish exactly.

The phase δ only plays a role if $\theta_{13} > 0$. Since θ_{13} is compatible with zero, no information on δ is available. We will see that this phase is of particular interest because it is responsible for CP violation, i.e., for neutrinos and antineutrinos to oscillate differently.

Within the current experimental precision, we have bi-tri-maximal mixing

$$\mathsf{U} = \frac{1}{\sqrt{6}} \begin{pmatrix} 2 & \sqrt{2} & 0 \\ -1 & \sqrt{2} & \sqrt{3} \\ 1 & -\sqrt{2} & \sqrt{3} \end{pmatrix} \quad \Rightarrow \quad \text{Probabilities} \begin{cases} \nu_1 = \frac{2}{3}\,\nu_e + \frac{1}{6}\,\nu_\mu + \frac{1}{6}\,\nu_\tau \\ \nu_2 = \frac{1}{3}\,\nu_e + \frac{1}{3}\,\nu_\mu + \frac{1}{3}\,\nu_\tau \\ \nu_3 = \qquad\quad \frac{1}{2}\,\nu_\mu + \frac{1}{2}\,\nu_\tau \end{cases}$$

10.2.2 Mass differences

Three flavors have three mass eigenstates, but oscillation experiments determine only mass-squared differences.

Solar and reactor oscillation experiments determine the "solar mass difference" to be

$$\Delta m^2_\odot = m^2_{21} = m^2_2 - m^2_1 = 75.9 \pm 2.0 \left({}^{+6.1}_{-6.9}\right) \ \text{meV}^2 \qquad \text{at } 1\,\sigma\text{, in brackets } 3\,\sigma$$

Atmospheric and accelerator long baseline experiments determine the "atmospheric mass difference" to be

$$\Delta m^2_{\text{atm}} = m^2_{31} = m^2_3 - m^2_1 = \begin{cases} -2400 \pm 110 \left({}^{+370}_{-390}\right) \ \text{meV}^2 \ \text{(inverted)} \\ +2510 \pm 120 \left({}^{+390}_{-360}\right) \ \text{meV}^2 \ \text{(normal)} \end{cases}$$

There remain two schemes, the normal or the inverted mass ordering, corresponding to

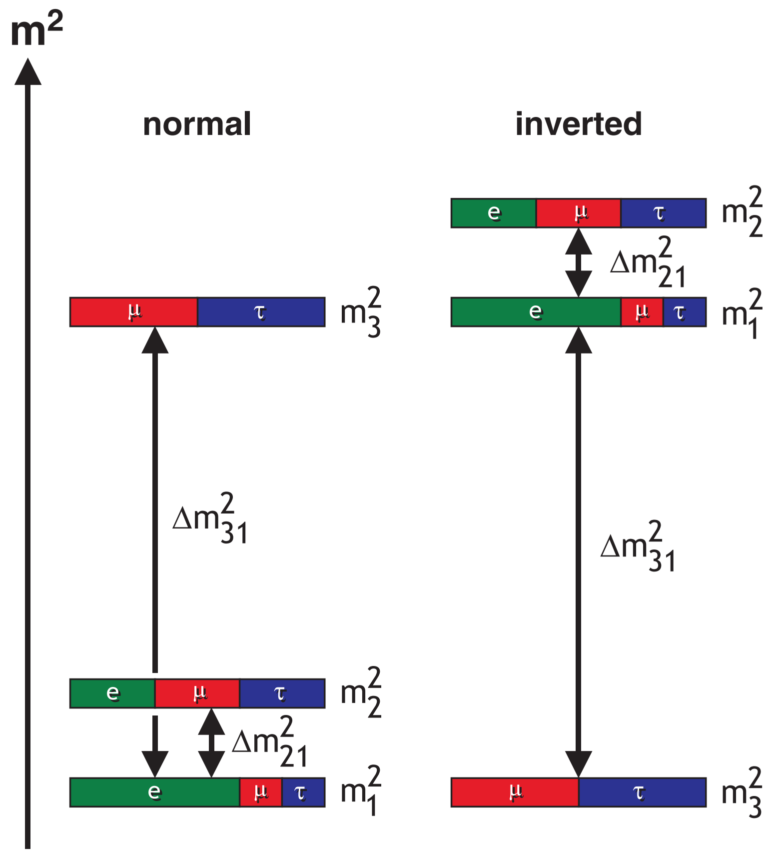

The solar mass ordering is fixed by the matter effect in the Sun (see later). Open questions:

- 13 mass ordering (normal vs. inverted)
- Absolute mass scale
- Dirac vs. Majorana

10.3 Two-flavor neutrino oscillations

Neutrino mixing parameters involve two small numbers:

- solar/atmospheric mass hierarchy parameter: $\alpha = \dfrac{\Delta m^2_\odot}{\Delta m^2_{\rm atm}} \sim \dfrac{1}{30}$
- $\sin^2\theta_{13} < 0.05$ at $3\,\sigma$

Therefore, there are two distinct very different length scales for oscillations. In the limit where $\theta_{13} = 0$, compatible with all data, oscillations fall into two distinct two-flavor blocks.

Study separately the "atmospheric" case of 2–3 oscillations and the "solar" case of 1–2 oscillations.

Historically, solar oscillations appeared first, but atmospheric oscillations are simpler (no matter effect) and were first to provide an unambiguous signature in 1998.

Recall the oscillation probability for a two-flavor system

$$p(\nu_\mu \to \nu_\tau) = \sin^2(2\theta)\,\sin^2\left(\frac{\Delta m^2}{4E}\,L\right) = \sin^2(2\theta)\,\sin^2\left(\pi\frac{L}{L_{\rm osc}}\right)$$

with L the distance traveled. The oscillation length is

$$\begin{aligned} L_{\rm osc} = \frac{4\pi E}{\Delta m^2} &= 991\ \text{km}\ \frac{(50\ \text{meV})^2}{\Delta m^2}\,\frac{E}{1\ \text{GeV}} \\ &= 248\ \text{km}\ \frac{(10\ \text{meV})^2}{\Delta m^2}\,\frac{E}{10\ \text{MeV}} \end{aligned}$$

The former is relevant for atmospheric and accelerator neutrinos, the latter for solar and reactor neutrinos.

Usually the neutrino sources have a broad spectrum of energies, leading to a smearing-out of the oscillation pattern after some distance.

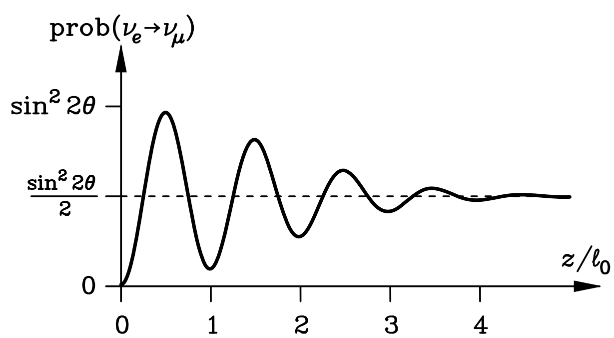

In this case oscillation effects are most apparent if we plot the survival probability as a function of the variable L/E, assuming the energy of every event can be separately measured.

10.4 Oscillations in the 2–3 sector

10.4.1 Atmospheric neutrino oscillations

Atmospheric neutrinos arise from primary cosmic rays (protons and heavier nuclei) interacting in the atmosphere, producing secondary particles, notably pions. Pion decay then produces secondary neutrinos according to

$$\pi^+ \to \mu^+ + \nu_\mu \to e^+ + \nu_e + \bar{\nu}_\mu + \nu_\mu$$
$$\pi^- \to \mu^- + \bar{\nu}_\mu \to e^- + \bar{\nu}_e + \nu_\mu + \bar{\nu}_\mu$$

Flavor ratio $e : \mu : \tau = 1 : 2 : 0$.

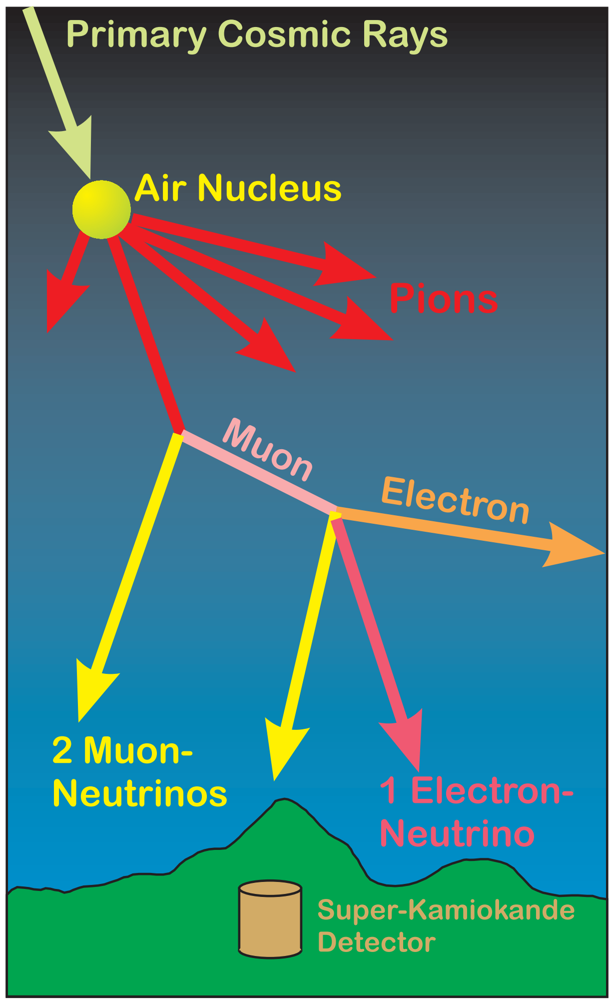

Atmospheric neutrinos have a steeply falling spectrum with typical detectable energies around 1 GeV.

How to detect these atmospheric neutrinos? Main method underground water Cherenkov detectors.

Cherenkov effect is the emission of photons by charged particles (electrons or muons) traveling in a transparent medium, notably water. The phase velocity of light is smaller than the speed of light if the refractive index $n > 1$ (space-like photons). In other words, the photon dispersion relation is

$$\omega^2 - k^2 = (1 - n^2)\omega^2 < 0$$

In this case the decay process of electron (or muon) into itself is kinematically allowed

$$e \to e + \gamma$$

In vacuum this process is forbidden by energy-momentum conservation.

It is a straightforward exercise to show that photons will be emitted with an angle θ relative to the electron direction given by

$$\cos\theta = \frac{1}{v_e n}$$

where v_e is the electron velocity, close to the speed of light for relativistic electrons, and n is the photon refractive index, approximately $n = 1.33$ in water. In this case the angle is roughly 41° for relativistic electrons.

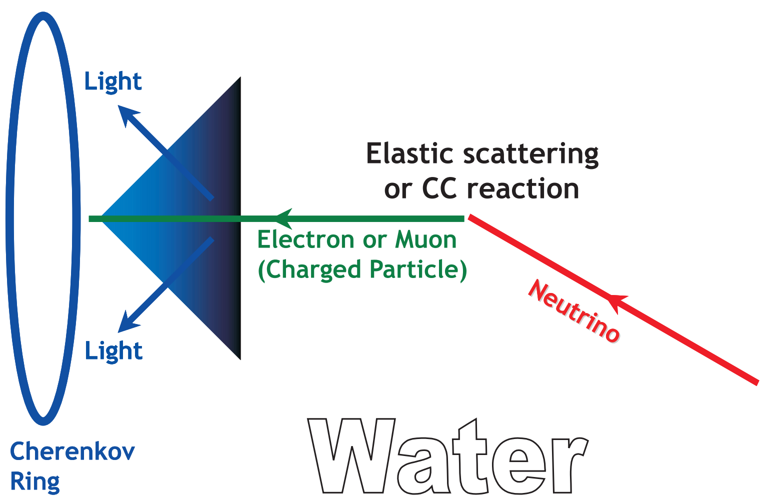

So an atmospheric neutrino produces an electron or a muon in a charged-current event of the form $\nu_e + n \to p + e^-$ and the secondary charged particle produces Cherenkov radiation.

Largest such detector (at relatively low energies) is Super-Kamiokande in Japan, consisting of 50 kton of purified water, surrounded by 12,000 photo multipliers. The detector is underground in a mine to shield against ordinary cosmic-ray muons.

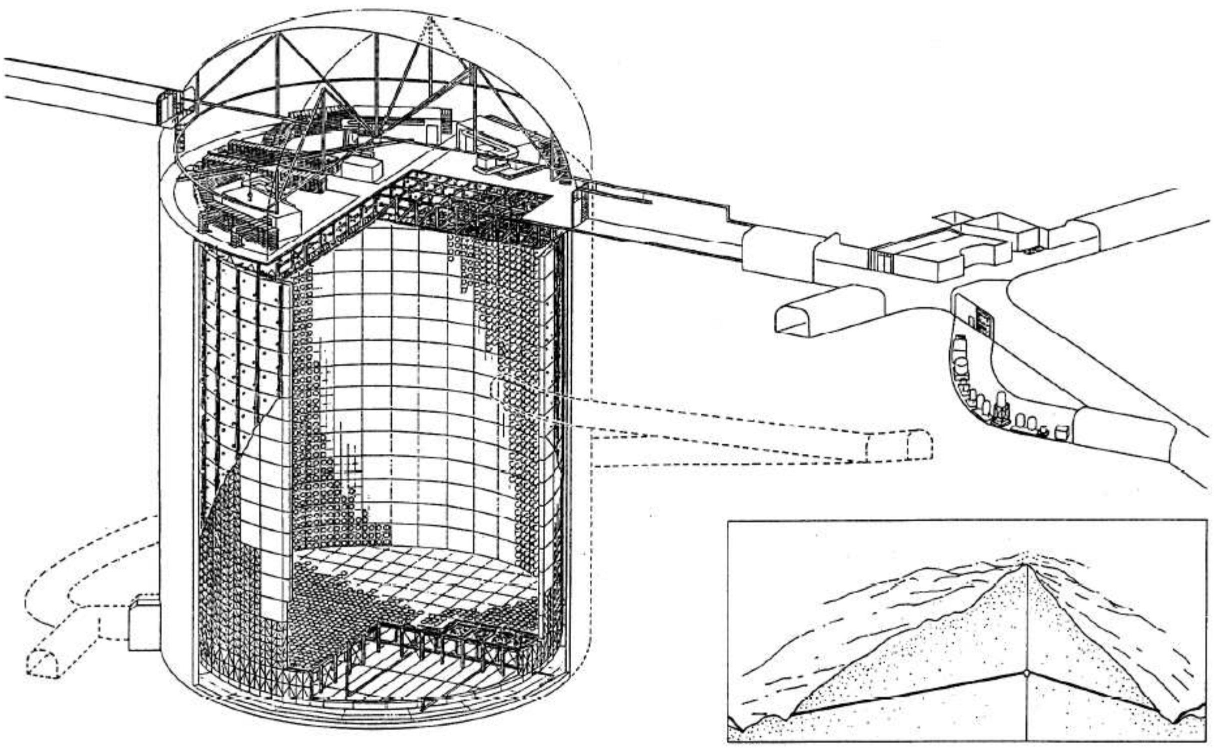

This detector is a multi-purpose neutrino observatory, being a workhorse for

- Solar neutrino detection
- Atmospheric neutrino detection
- Search for proton decay
- Search for neutrinos from dark-matter annihilation in the Sun or Earth
- A galactic supernova neutrino burst would be detected with a huge signal (approx. 10^4 events)

The detector took up operations on 1 April 1996 and has been taking data since with some interruptions.

The famous picture from filling the detector is here:

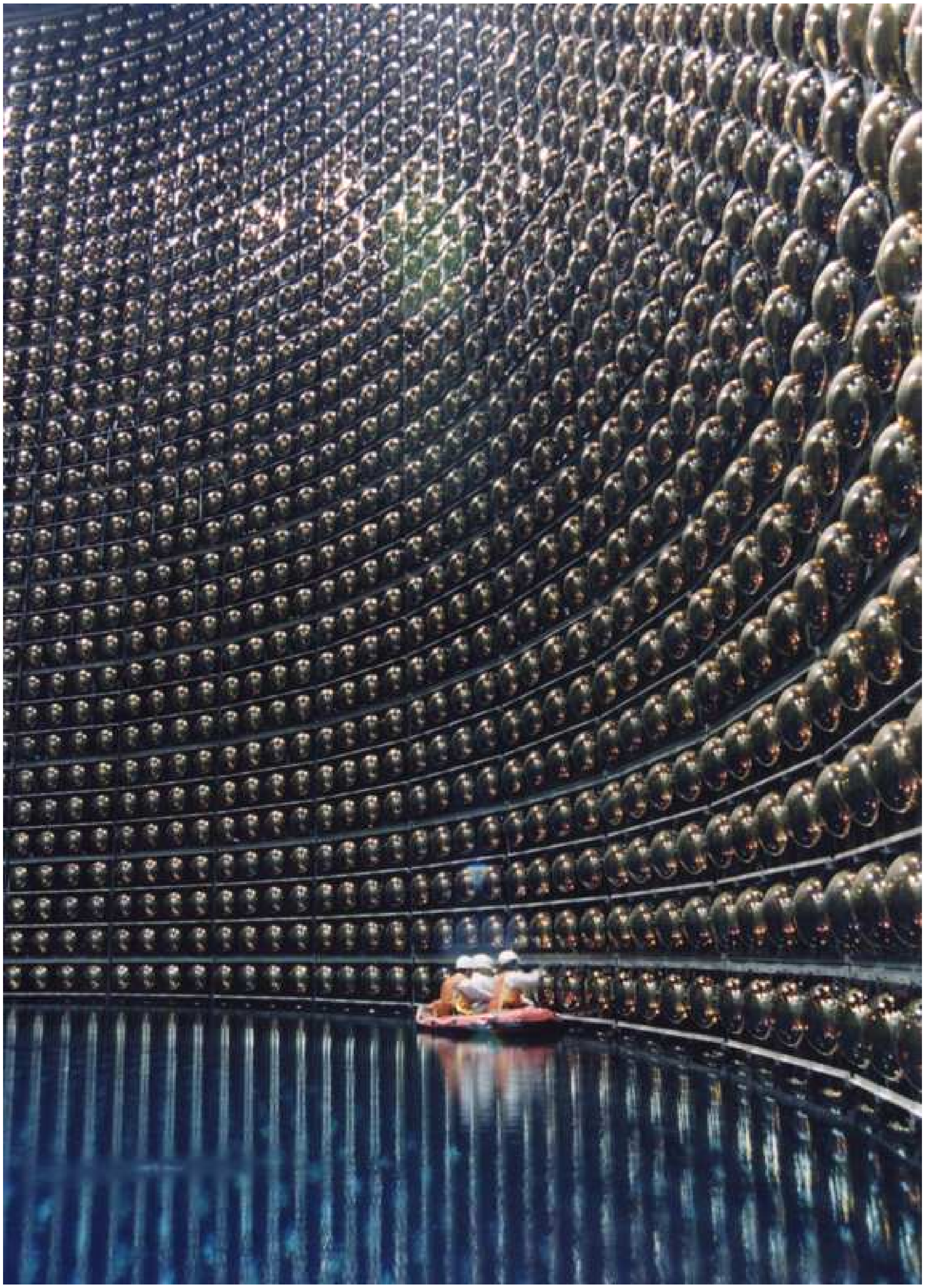

To discover neutrino oscillations we need to distinguish between electron- and muon-flavor neutrinos. This is achieved by noting that electrons, because of their smaller mass, are deflected more in the interactions with the Coulomb fields of the water constituents. Therefore, an electron causes a more fuzzy Cherenkov ring than a muon.

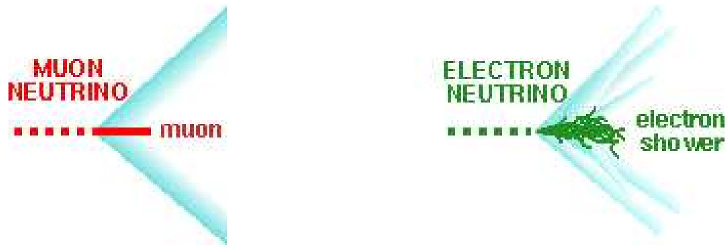

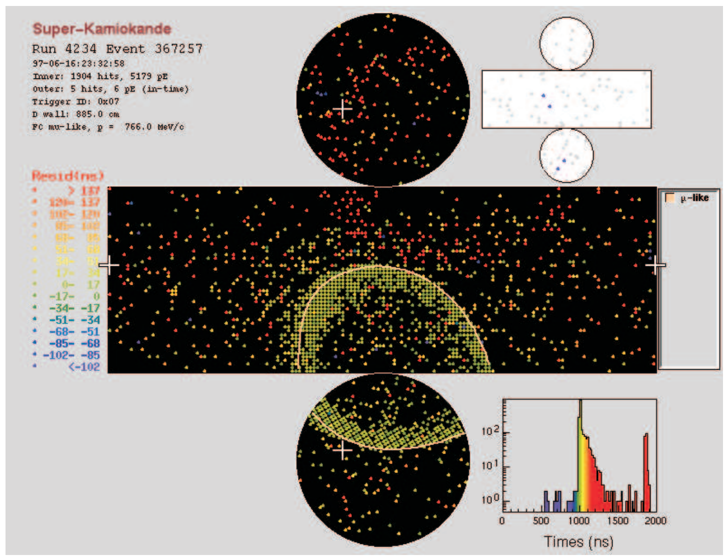

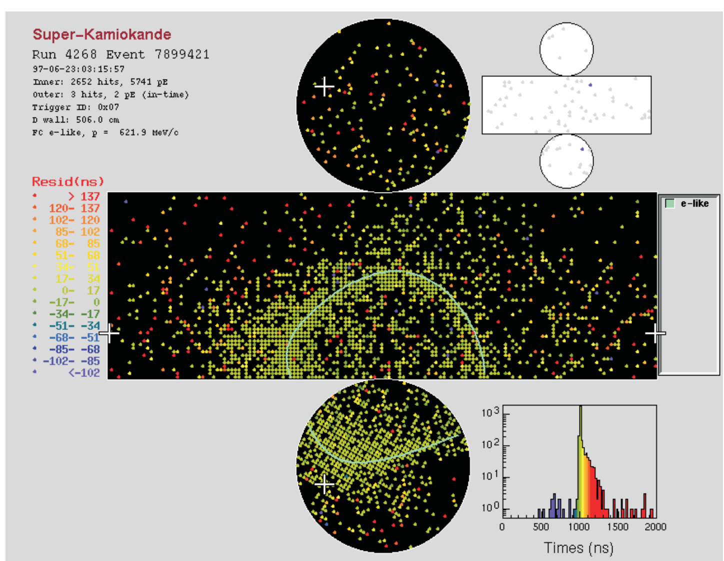

Super-Kamiokande measures neutrinos from all around the Earth, with roughly equal fluxes per solid angle for every direction. The neutrinos from the other side of the Earth suffer a $1/r^2$ geometric flux dilution, but there is r^2 more atmosphere in a given solid angle.

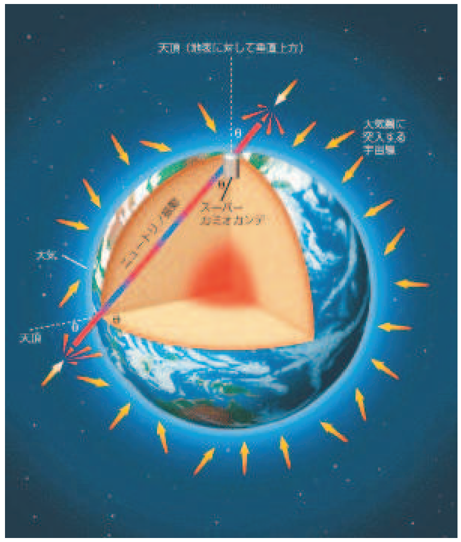

Early on, the Kamiokande detector, predecessor of Super-K, observed an up/down asymmetry of the μ/e flavor ratio: One motivation to build Super-K.

Once Super-K took data, very quickly the effect could be measured in detail and evidence for atmospheric neutrino oscillations was published in 1998. Today, with more data, the zenith-angle distribution for μ-flavor neutrinos looks like this

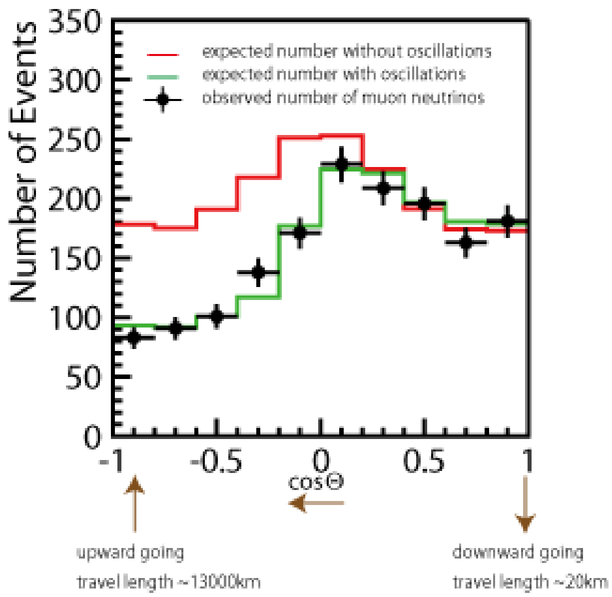

For e-flavor neutrinos it is unchanged. So the oscillation channel must be $\nu_\mu \to \nu_\tau$: Disappearance of ν_μ, but no appearance of excess ν_e.

In the down-direction one loses roughly half the flux, so the mixing must be close to maximal. The oscillation length must be of order a few 1000 km. This implies the mass-squared difference of order $(50\ \mathrm{meV})^2$ discussed earlier.

Since the energy spectrum is broad, oscillation features are best seen in an L/E diagram. The histogram shows the expected modulation of the μ-flavor rate, including energy and directional resolution effects that causes some smearing. This is compared with the data (from arXiv:hep-ex/040403).

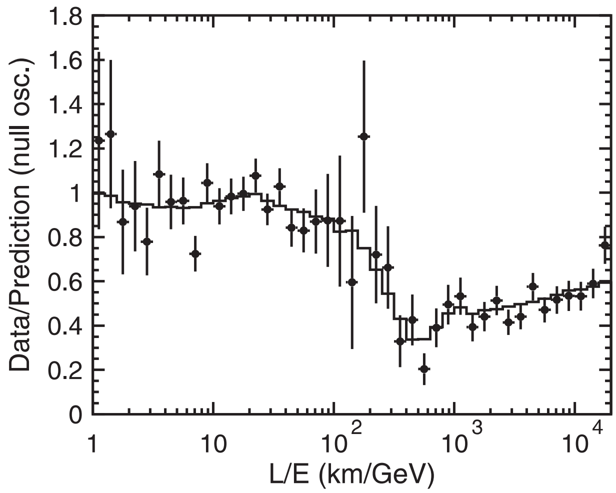

Allowed range of oscillation parameters (at 90%, 95%, 99%, and 99.73% CL) from the atmospheric data (full colored regions, best fit marked with a star) and from long-baseline accelerator data (solid contours, best fit marked with a circle), from arXiv:1001.4524.

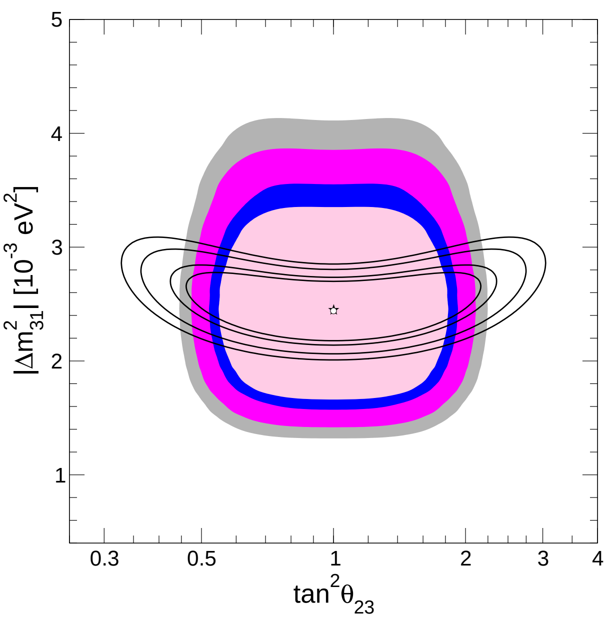

10.5 Long-baseline accelerator experiments

10.5.1 K2K Experiment

The atmospheric neutrino oscillation effect can also be tested using a neutrino beam made in an accelerator. First experiment was K2K in Japan, a beam over 250 km across Japan from the KEK laboratory to the Super-Kamiokande detector.

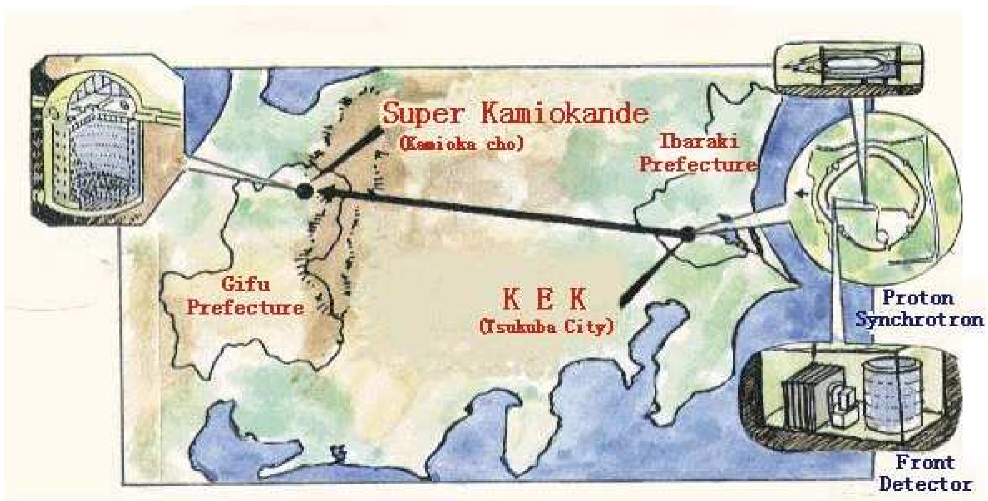

A neutrino beam is made in the same way as atmospheric neutrinos. In principle, one proceeds as follows:

- Accelerate protons, at K2K experiment to 12 GeV
- Let proton beam hit a target, e.g. a block of metal
- Secondary pions are produced, notably π^+
- First decay $\pi^+ \to \mu^+ + \nu_\mu$ in a decay tunnel, produces ν_μ beam because of relativistic boost
- Second decay $\mu^+ \to e^+ + \nu_e + \bar{\nu}_\mu$ takes a long time, so μ^+ can be blocked by a beam dump to produce an almost pure ν_μ beam.

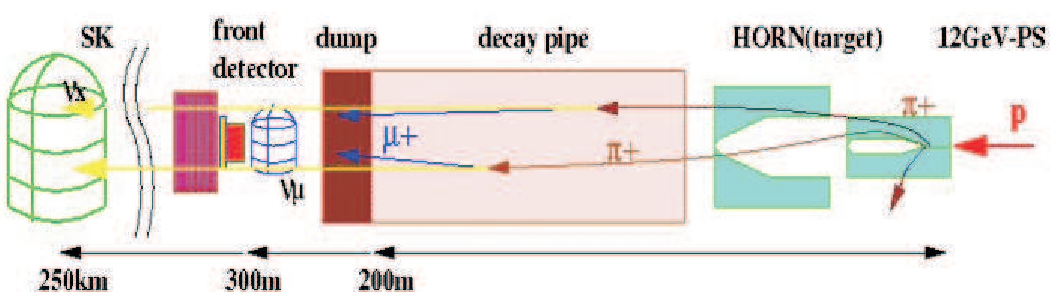

Experiment is of disappearance type:

- Measure beam at near detector
- Compare with flux at far detector and look for disappearing ν_μ

The mean neutrino energy of 1.3 GeV is too small to produce τ leptons after oscillations, so only disappearance possible. (Note: $m_\tau = 1.777$ GeV)

Data taken from 1999–2004 confirmed the atmospheric results—for common fit see figure above.

10.5.2 Minos

The next accelerator experiment is the MINOS experiment with the NuMI beam from Fermilab near Chicago to the Soudan mine with the MINOS detector. Primary protons: 120 GeV. Neutrino beam: up to 50 GeV, Maximum at 3.5 GeV.

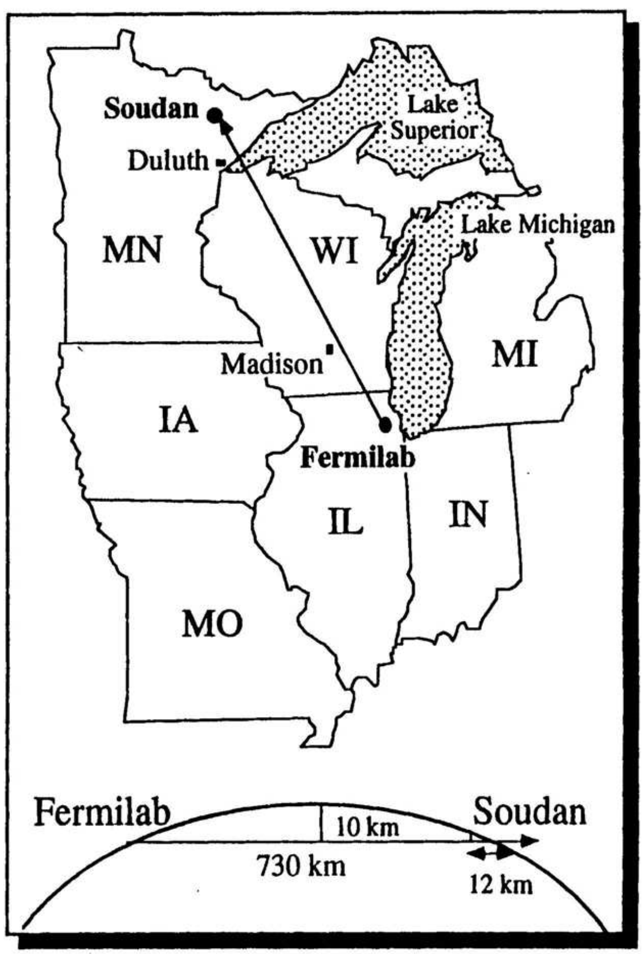

Most recent result, comparing expected with measured ν_μ flux at the far site.

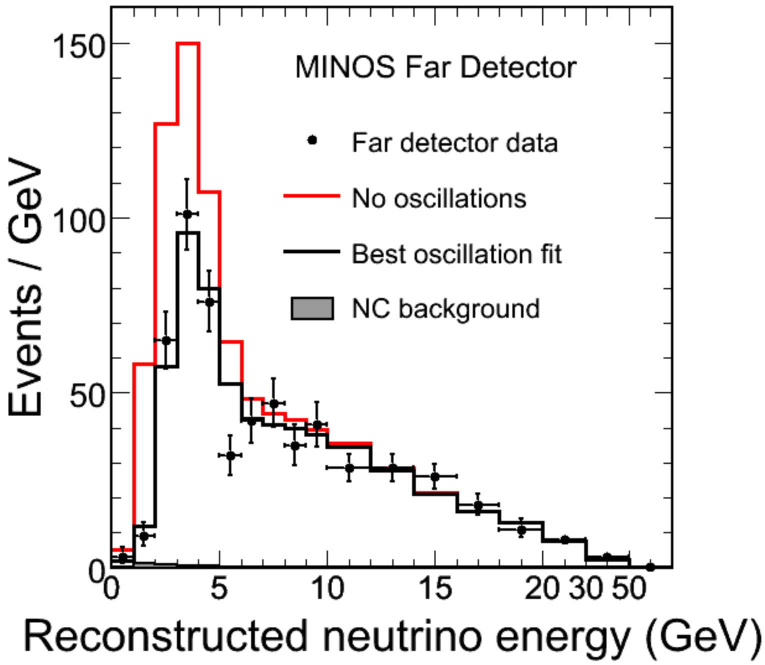

10.5.3 CNGS Experiment and Opera Detector

The ongoing CERN to Gran Sasso experiment, also a baseline of 735 km, has a detector that can resolve τ decays and could detect τ appearance from $\nu_\mu \to \nu_\tau$ oscillations. No results have been reported yet.

Other long-baseline experiments are in preparation for high-intensity beams to search for subdominant oscillation channels, notably in a three-flavor treatment (see later).

10.6 Solar neutrinos

Historically the first evidence for neutrino oscillations was found in the late 1960s and later in the form of the "solar neutrino problem" or the "missing ν_e flux" from the Sun.

The Sun produces energy by nuclear fusion of hydrogen into helium by the effective reaction

$$4p + 2e^- \to {}^4\text{He} + 2\nu_e + 26.73 \text{ MeV}$$

With a total luminosity of

$$L_\odot = 3.85 \times 10^{33} \text{ erg s}^{-1} = 2.4 \times 10^{39} \text{ MeV s}^{-1}$$

the Sun produces about

$$1.8 \times 10^{38} \ \nu_e \text{ s}^{-1}$$

and thus at a distance of 150 million km a flux at Earth of

$$F_{\nu_e} = 6.6 \times 10^{10} \text{ cm}^{-2} \text{ s}^{-1}$$

The spectrum is determined by the relative importance of different nuclear reaction chains, notably the pp chains.

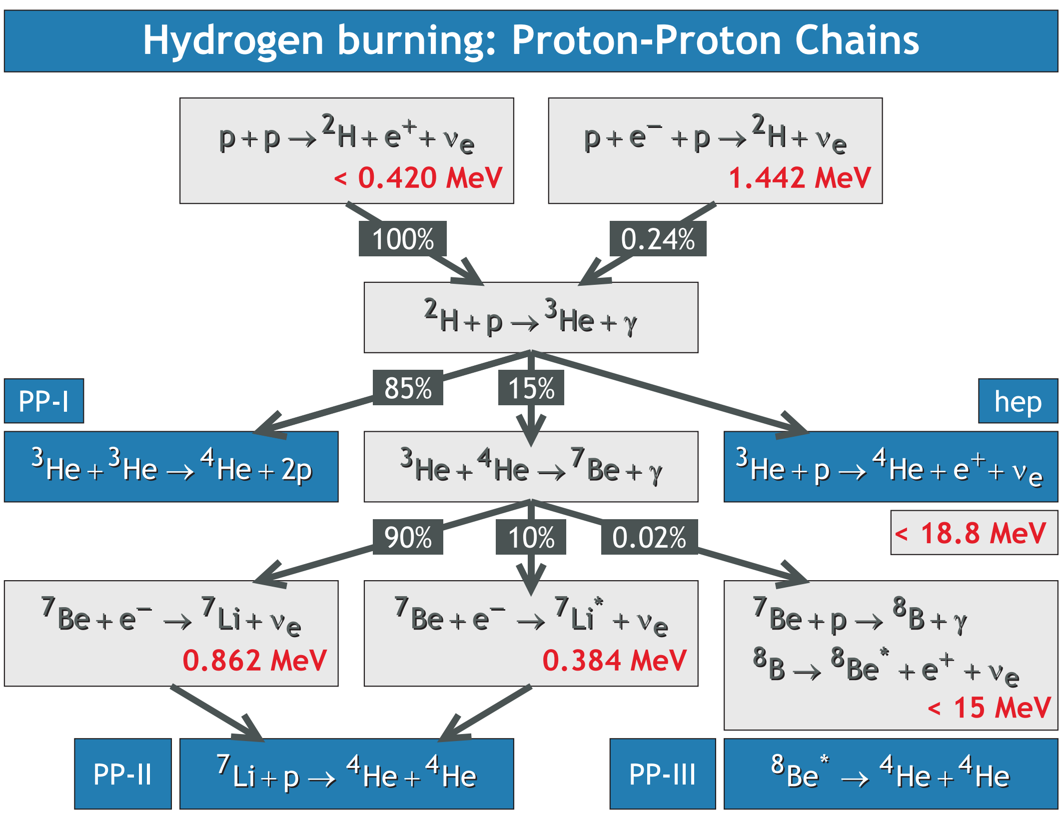

The resulting spectra are calculated to be of the following form

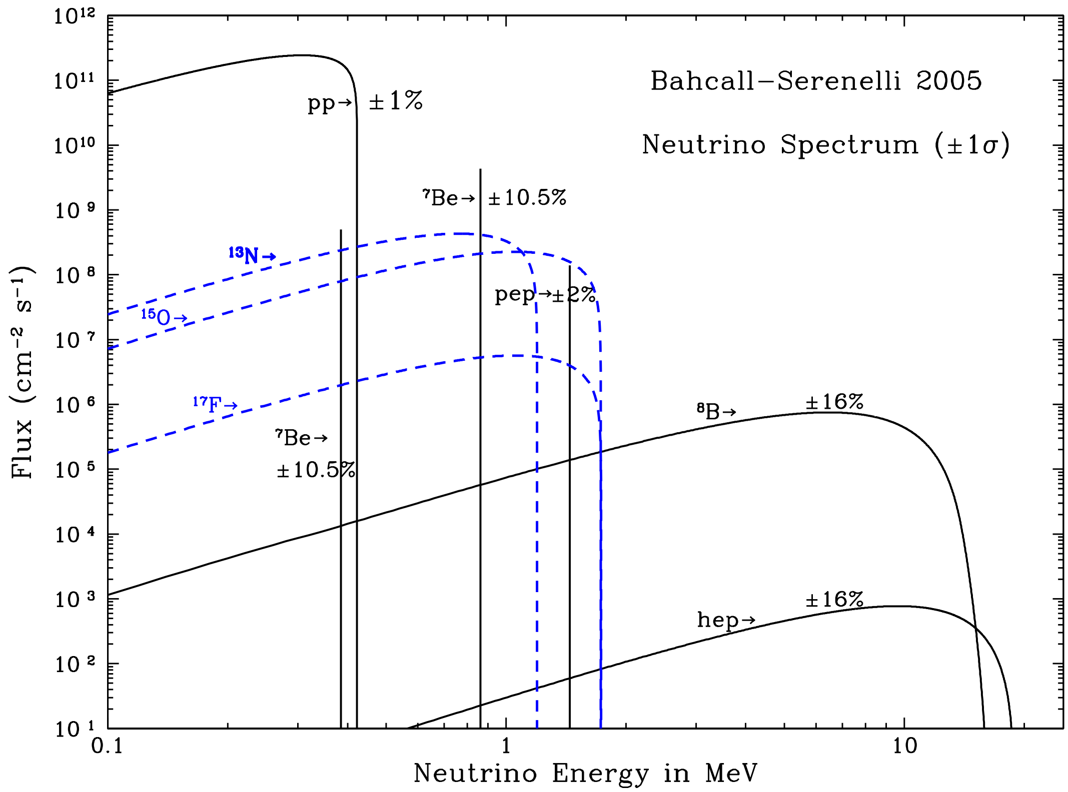

The oldest solar neutrino experiment is the pioneering experiment by Ray Davis (1914–2006) in the Homestake mine and for which he received the physics Nobel prize in 2002. It is based on the reaction

$$\nu_e + {}^{37}\mathrm{Cl} \to {}^{37}\mathrm{Ar} + e \qquad \text{threshold } 0.814 \text{ MeV}$$

The experiment used 600 tons of perchloroethylene (a cleaning fluid and therefore cheap). The experiment ran from 1967–2002.

The production rate is a few argon atoms per month. They had to be washed out from the tank, concentrated, and finally counted: They are themselves unstable and decay with a half-life of 35 days back to chlorine

$$e^- + {}^{37}\mathrm{Ar} \to {}^{37}\mathrm{Cl} + \nu_e$$

The data were very noisy, yet clearly showed a large deficit of the expected flux.

Depending on the exact solar model, the predicted flux in Solar Neutrino Units (SNU) is 8.1 ± 1.2, but depends sensitively on temperature and production cross section. (1 SNU = 10^{-36} s^{-1} absorptions per target nucleus.)

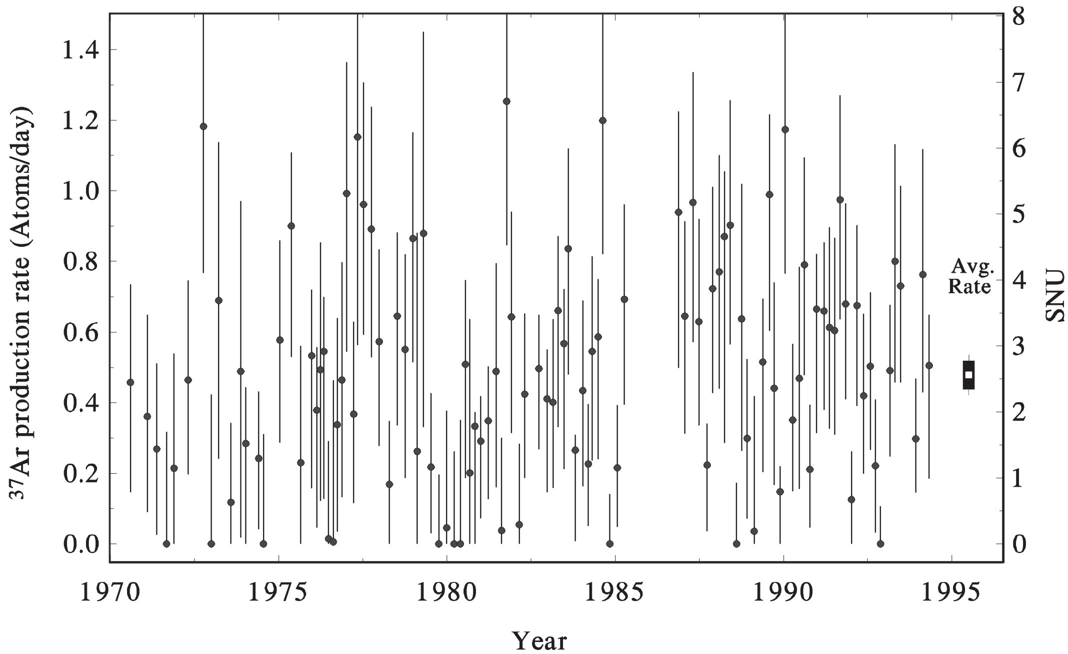

A later class of radiochemical experiments used gallium instead of chlorine, based on the reaction

$$\nu_e + {}^{71}\text{Ga} \to {}^{71}\text{Ge} + e \qquad \text{threshold } 0.233 \text{ MeV}$$

There were two such experiments: SAGE in Russia, producing data since 1990, and GALLEX, later GNO, taking data since 1991, and meanwhile decommissioned. They again measured a deficit of ν_e. They picked up part of the dominant low-energy *pp* neutrino flux, so the deficit seemed more credible.

The next type of solar neutrino experiment is a water Cherenkov detector, where the original Kamiokande detector, the predecessor of Super-K, began data taking in 1987. Here one detects neutrinos by elastic scattering on electrons

$$\nu + e \to e + \nu$$

One measures the Cherenkov photon emission of the recoiling electron.

Because of backgrounds, the analysis threshold was around 7 MeV, so one picked up only the high-energy ^{8}B neutrino flux.

Later the Super-Kamiokande detector measured the flux with far greater precision (since 1996). The electron recoil allows for a crude angular resolution.

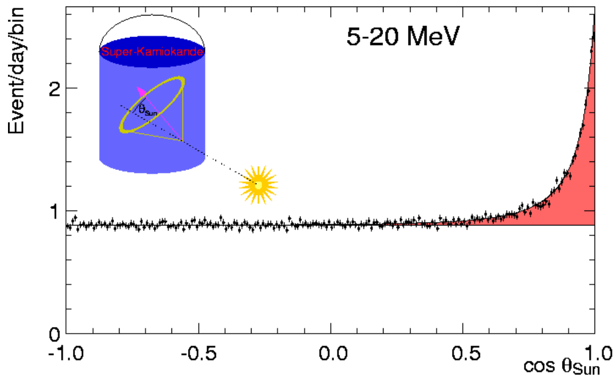

As a result, the neutrino events allowed one to construct a false-color image of the Sun in the light of neutrinos in the sky.

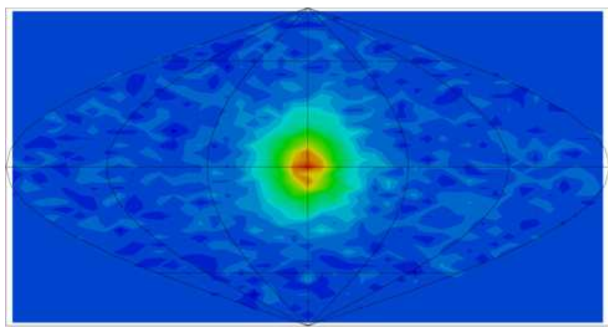

Actually one can see in the total measured flux the annual variation due to the distance variation from the Sun (elliptic Earth orbit).

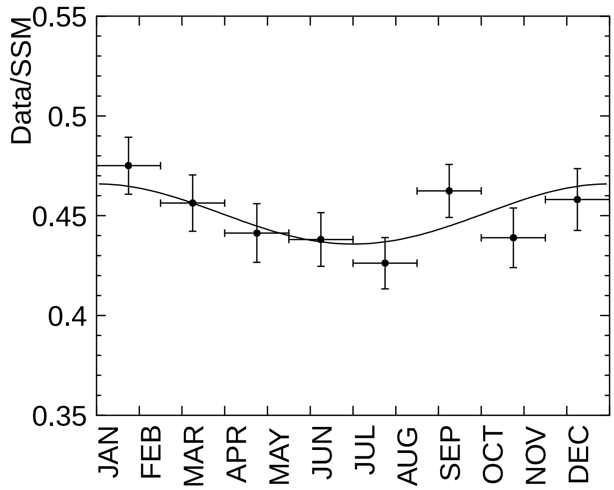

The electron-scattering reaction occurs for all flavors, but with a different cross section because ν_e scattering on e also occurs by W exchange.

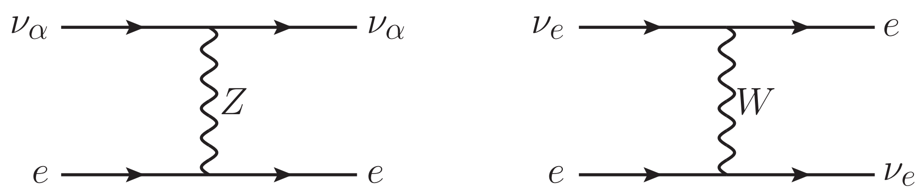

The cross section for $\nu_{\mu,\tau}$ scattering is roughly 1/7 that of ν_e, so very roughly the rate is dominated by ν_e.

The water Cherenkov experiments once more confirmed the "missing" flux of solar ν_e.

The most important clarification came from the Sudbury Neutrino Observatory (SNO). It used 1000 tons of heavy water (D_2O) and thus had several detection channels available

$\nu_\alpha + e \to e + \nu_\alpha$	ES, mostly ν_e
$\nu_e + d \to p + p + e$	CC
$\nu_\alpha + d \to p + n + \nu_\alpha$	NC, all flavors equally

Therefore, the flux Φ_e of electron neutrinos and $\Phi_{\mu\tau}$ of the other flavors could be separately measured.

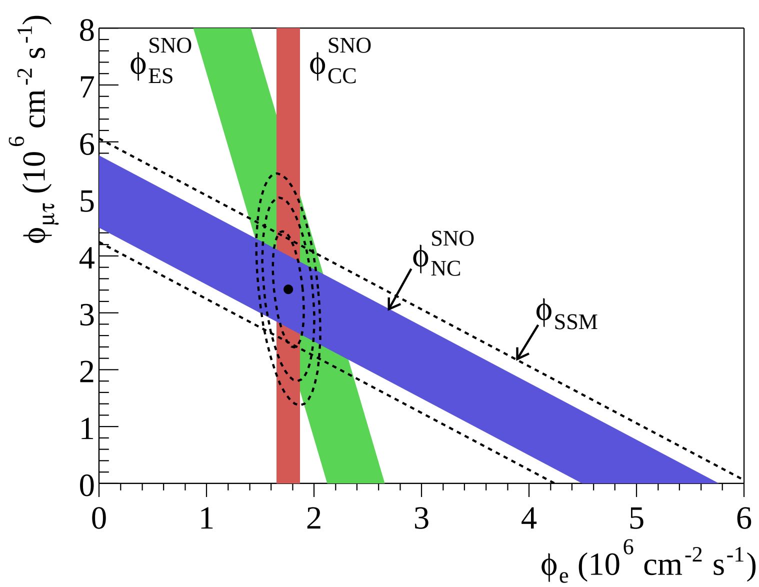

Therefore, one could measure the all-flavor flux, confirming that no neutrinos were missing, but that they had converted from ν_e to other flavors (published in 2002).

The overall picture that emerged from all solar neutrino measurements is summarized here.

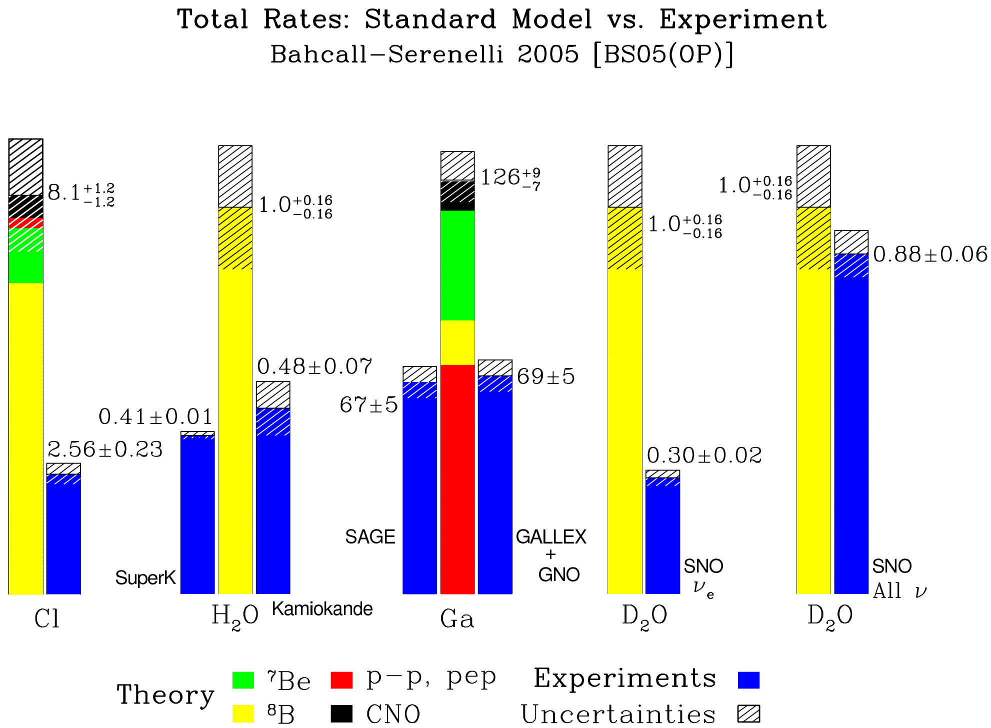

The effective flux reduction is different in different experiments, corresponding to the different energy window covered by a detector. The interpretation requires taking into account matter effects on neutrino oscillations in the Sun (see below). The current best fit is given by the colored contours (arXiv:1001.4524).

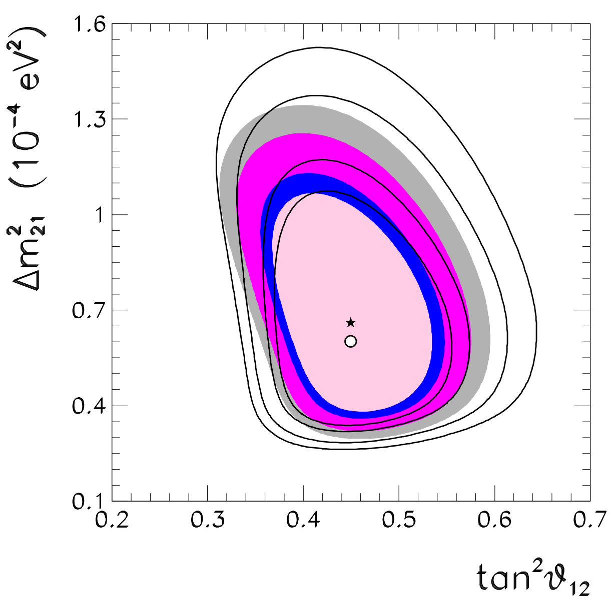

10.7 Oscillation in matter

Neutrinos suffer a refractive index in a medium, and this effect is crucial for the interpretation of solar neutrino oscillations.

The neutrino interaction by Z and W exchange effectively implies a potential for neutrinos in a medium, just as electrons would feel a potential in an electrically charged environment.

This potential is different for ν_e and $\nu_{\mu,\tau}$ because of W exchange graph (see above). The effective shift of the energy is given by

$$E \to E - V \qquad \text{where} \qquad V = \pm\sqrt{2}\, G_{\rm F} \times \begin{cases} n_e - \frac{1}{2}\, n_n & \text{for } \nu_e \\ -\frac{1}{2}\, n_n & \text{for } \nu_{\mu,\tau} \end{cases}$$

The upper sign is for neutrinos, the lower for antineutrinos.

Linearized Klein-Gordon eqn for neutrinos in a medium, assuming a chosen energy mode E, in analogy to the axion-photon mixing case

$$\mathrm{i}\partial_z \Psi = \left(-E + \mathsf{V} + \frac{\mathsf{M}^2}{2E}\right)\Psi$$

where in the weak interaction basis

$$\Psi = \begin{pmatrix} \nu_e \\ \nu_\mu \\ \nu_\tau \end{pmatrix} \qquad \text{and} \qquad \mathsf{V} = \sqrt{2}\, G_{\rm F} \begin{pmatrix} n_e & 0 & 0 \\ 0 & 0 & 0 \\ 0 & 0 & 0 \end{pmatrix} - \frac{1}{2}\, n_n$$

and the mass-squared matrix is in the weak interaction basis

$$\mathsf{M}^2 = \mathsf{U}^\dagger \begin{pmatrix} m_1^2 & 0 & 0 \\ 0 & m_2^2 & 0 \\ 0 & 0 & m_3^2 \end{pmatrix} \mathsf{U}$$

As usual, we may remove pieces of the matrices that are proportional to the unit matrix because they only contribute a common phase.

In the two-flavor case the linearized wave equation then takes on the form

$$\mathrm{i}\partial_z \Psi = \mathsf{H}\Psi \qquad \text{where} \qquad \mathsf{H} = -\frac{\Delta m^2}{4E} \begin{pmatrix} \cos 2\theta & \sin 2\theta \\ \sin 2\theta & -\cos 2\theta \end{pmatrix} + \frac{G_{\rm F} n_e}{\sqrt{2}} \begin{pmatrix} 1 & 0 \\ 0 & -1 \end{pmatrix}$$

Consider an ordinary medium where the electron density is half the baryon density:

$$\frac{G_{\rm F} n_e}{\sqrt{2}} = 1.91 \times 10^{-14}\ \text{eV}\ \frac{\rho}{\text{g cm}^{-3}}$$

$$\frac{\Delta m^2}{4E} = 2.5 \times 10^{-12}\ \text{eV} \frac{\Delta m^2}{(10\ \text{meV})^2}\ \frac{10\ \text{MeV}}{E}$$

Matter density near the solar center around 100 g cm^{-3}, so for higher-energy solar neutrinos the matter effect is important relative to the vacuum masses!

If the medium is much denser than in the Sun (e.g. in a supernova core) or if the energy is much higher, matter effect suppresses neutrino mixing: The interaction eigenstate roughly coincides with the propagation eigenstate.

In general, the propagation eigenstates are found from diagonalizing the matrix H. Straightforward calculation yields the mixing angle in the medium in terms of the vacuum mixing angle θ_0 as

$$\tan 2\theta = \frac{\sin 2\theta_0}{\cos 2\theta_0 - \xi}$$

$$\sin 2\theta = \frac{\sin 2\theta_0}{\sqrt{\sin^2 2\theta_0 + (\cos 2\theta_0 - \xi)^2}}$$

where

$$\xi = \frac{\sqrt{2} G_{\rm F} n_e 2E}{\Delta m^2} = 1.53 \, \frac{Y_e \rho}{100 \text{ g cm}^{-3}} \, \frac{E}{10 \text{ MeV}} \, \frac{(10 \text{ meV})^2}{\Delta m^2}$$

with Y_e the number of electrons per baryon.

The dispersion relation has two branches which in vacuum correspond to

$$E_{1,2} = \sqrt{p^2 + m_{1,2}^2}$$

In the presence of a medium they are in the relativistic limit

$$E_{1,2} - p = \frac{m_2^2 + m_1^2}{4E} + \sqrt{2}\, G_{\rm F} n_B \left(Y_e - \frac{1}{2}\right) \pm \frac{m_2^2 - m_1^2}{4E} \sqrt{\sin^2 2\theta_0 + (\cos 2\theta_0 - \xi)^2}$$

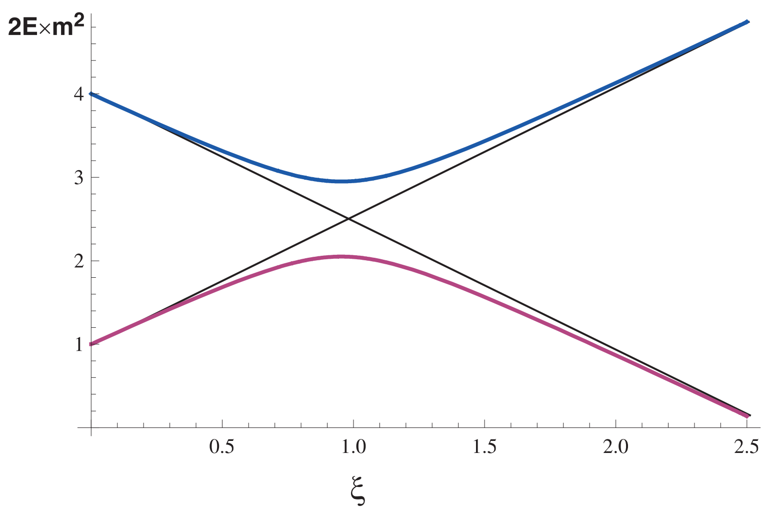

Note that the eigenvalues of a Hermitean matrix as a function of a parameter never cross, they “repel.” The smaller the mixing angle, the “sharper” the cross over, i.e., the closer they get.

Same effect, for example, in the mixing of atomic levels by, say, an external B-field.

At vanishing density ($\xi = 0$), the propagation eigenstates equal the mass eigenstates. At high density, they equal the interaction eigenstates.

Assume the density profile varies “slowly” and that a neutrino is produced at high density: The propagation eigenstate is, say, almost equal to the ν_e, so no oscillations. As the density decreases along the trajectory, the propagation eigenstate slowly turns into mass eigenstates, following the branch on the dispersion relation, ending in vacuum (outside of the Sun) as a mass eigenstate.

If the density changes too quickly (non-adiabatic), the state follows the “black lines” and jumps over the level crossing, as if the levels would cross. This happens when the levels get very close, i.e. for a small mixing angle.

For solar neutrinos, there are three regimes for a fixed mixing angle and fixed Δm^2.

- Small energy: The density in the Sun is too low for a level crossing, and we have effective vacuum oscillations, no resonance.
- Intermediate energy: Adiabatic level crossing, almost full conversion.
- Large energy: Nonadiabatic level crossing, and hardly any flavor conversion.

As a function of energy, one obtains the bathtub picture of survival probability in the Sun for neutrinos produced at its center (curves marked with $\sin^2 2\theta$).

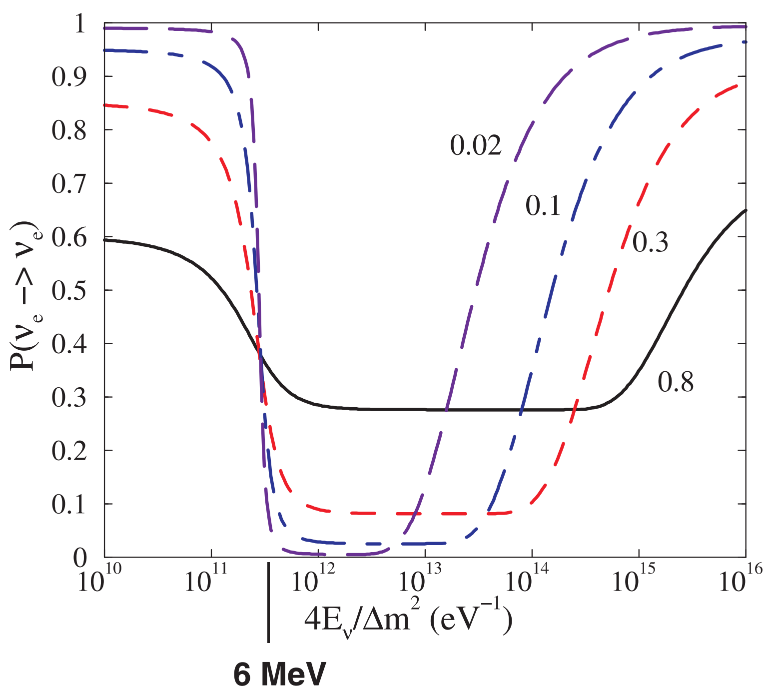

Originally, this MSW effect was thought to be very important to explain a large conversion effect for an assumed small mixing angle (as for quarks). Today we know that the mixing angle is large.

Still, matter effect crucial to explain energy-dependent conversion efficiency and to determine mass ordering between 1 and 2 states. (No level crossing for inverted hierarchy).

10.8 Reactor neutrino oscillations (Kamland)

The solar mixing angle is large and the oscillation length for MeV neutrinos of order a few 100 km.

It becomes thinkable to use $\bar{\nu}_e$ from a power reactor to search for solar neutrino oscillations.

This was done by the Kamland experiment: A 1 kton liquid scintillator detector in the underground cavern that originally housed the Kamiokande experiment.

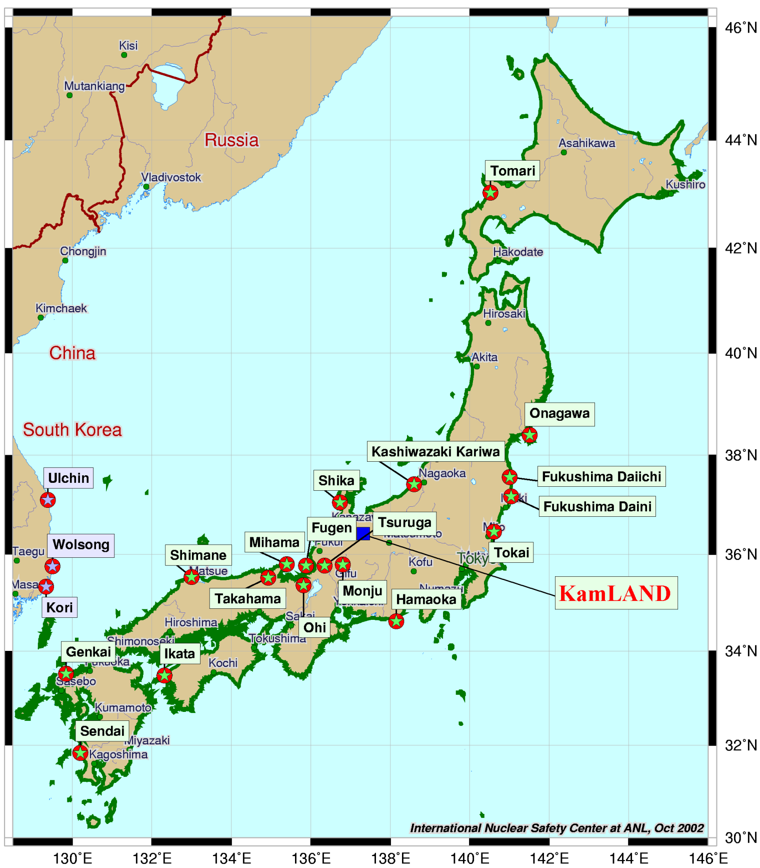

Average distance to most powerful reactors: 180 km. About 80 Gigawatts thermal power, roughly 20% of the world's installed nuclear power.

Per nuclear fission, about 200 MeV of energy is released (roughly 1 MeV per nucleon). So this nuclear power corresponds to

$$\text{Fission rate} = \frac{80 \text{ GW}}{200 \text{ MeV}} = 2.5 \times 10^{21} \text{ s}^{-1}$$

The neutrino spectrum per nuclear fission is given here.

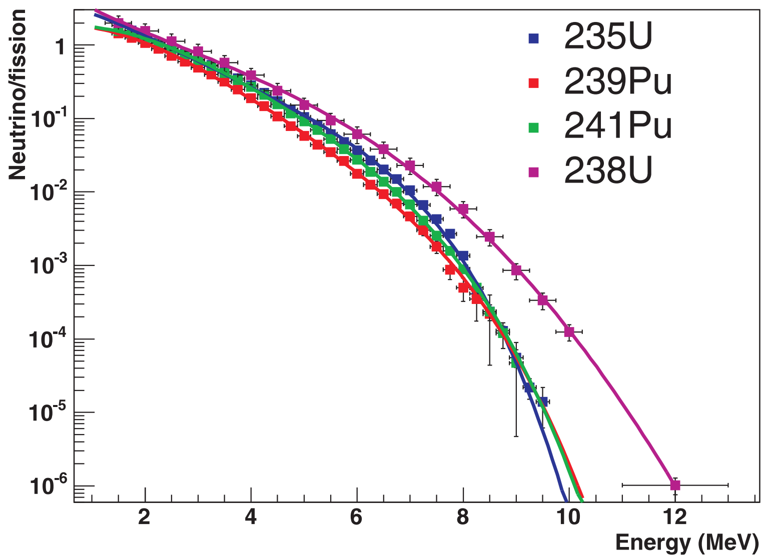

The energy spectrum falls quickly. So per fission one has about 1 detectable neutrino. Therefore flux of detectable neutrinos at the distance of 180 km

$$F_{\text{Kamland}} \sim 6 \times 10^5 \text{ cm}^{-2} \text{ s}^{-1}$$

This corresponds to something like 2 $\bar{\nu}_e$ detections per day from $\bar{\nu}_e + p \to n + e^+$ (inverse beta decay).

First data were taken in 2002 and the oscillation effect was measured. in the form of an L/E plot one can today beautifully see the oscillation pattern.

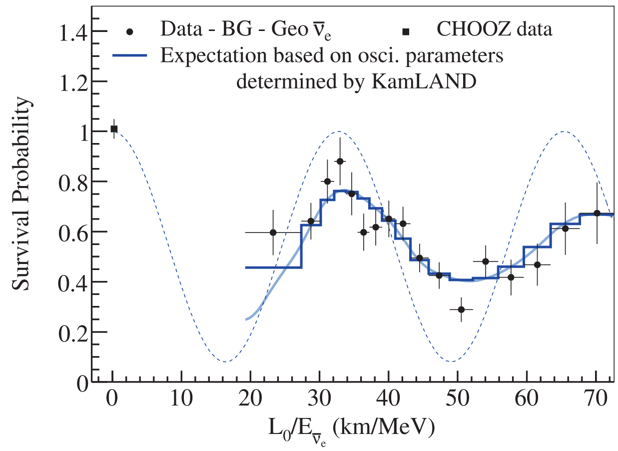

Common fit of Kamland and solar data together pin down the solar mixing parameters with great precision.

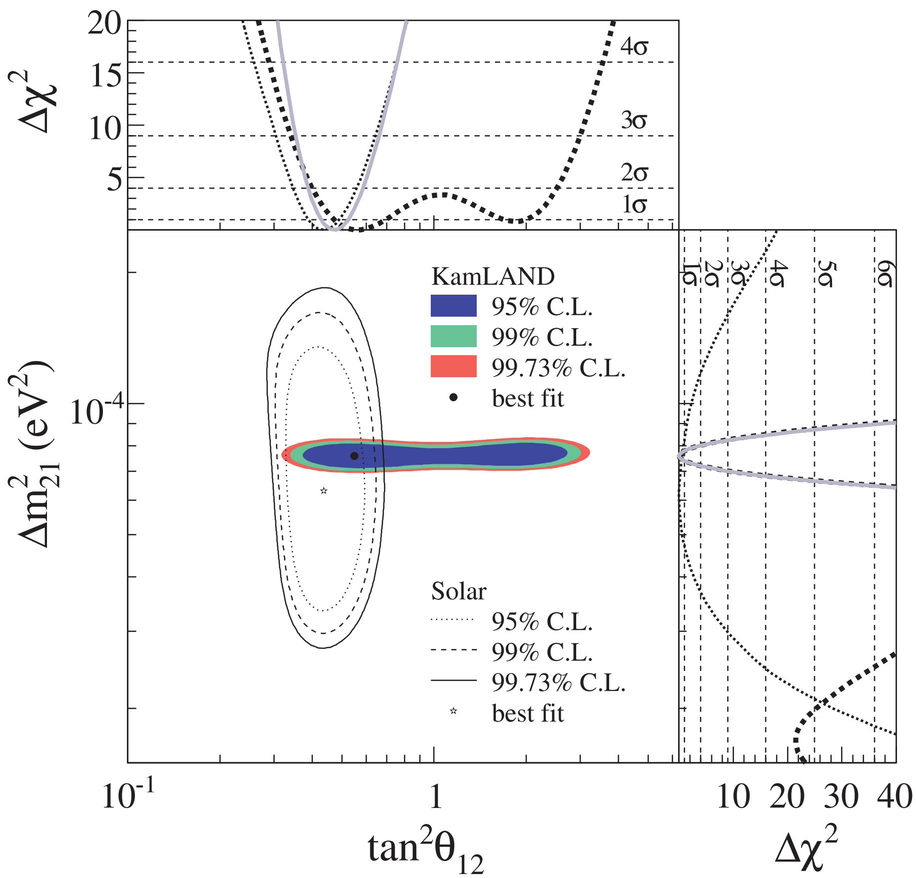

10.9 Subdominant three-flavor oscillations: Chasing θ_{13}

Oscillations in the 1–2 sector and in the 2–3 sector treated separately as two-flavor oscillations because the 1–3 mixing angle is small.

However, if it is non-zero, the $\bar{\nu}_e$ survival probability as a function of distance has two frequencies in it, driven by $\Delta m^2_{\odot}$ and by $\Delta m^2_{\rm atm}$.

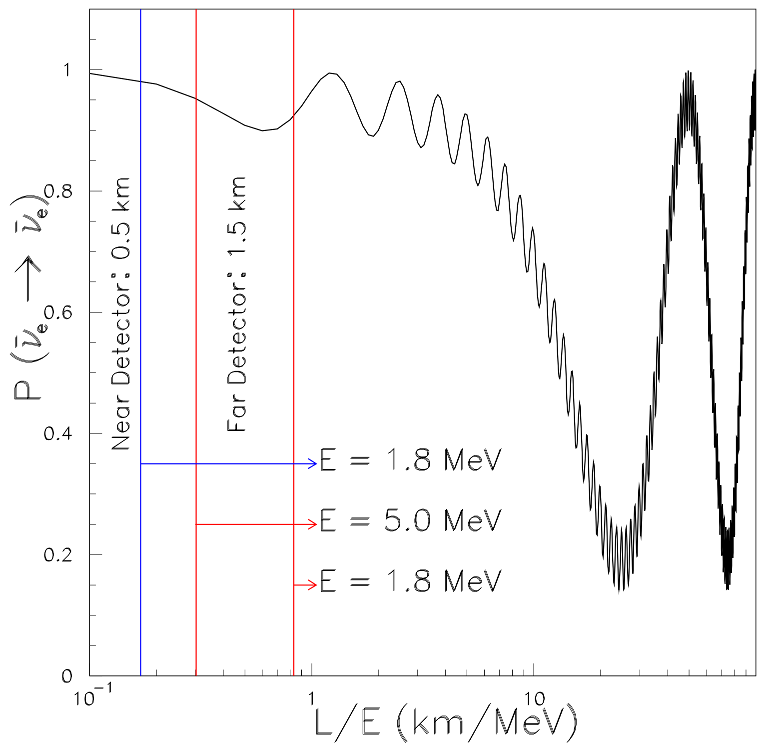

For reactor neutrinos with maximum of detection spectrum at about 3–4 MeV, optimal length for subdominant 1–3 oscillation at 1–2 km distance.

Effect is small, so systematic errors crucial limitation. Need a near detector (to measure exact reactor output) and far detector at 1–2 km.

Three experiments getting close to taking data: Double-Chooz experiment (France), Daya-Bay (China) and Reno (Korea). Can find θ_{13} if it is "just around the corner."